Derivation of kinetic coefficients by atomistic methods for studying defect behavior in Mo

Z. Insepov,* J. Rest, A. Yacout
Argonne National Laboratory, Argonne, Illinois, USA
A. Yu. Kuksin, G. E. Norman, S. V. Starikov, V. V. Stegailov, A. V. Yanilkin
Joint Institute for High Temperatures, Russia

ABSTRACT
A new multiscale concept is formulated based on coupling ab initio and atomistic molecular dynamics simulations with kinetic mesoscale models. The parameters of the atomistic and kinetic models are obtained from ab initio density-functional theory calculations, and the results are then compared with results from models based on kinetic rate theory. The evolution of a system containing self-interstitial atoms (SIAs) and vacancies in crystalline molybdenum is investigated. Fundamental radiation enhanced defect processes are studied, namely, the formation of di-SIAs and recombination of defects. The effects of temperature and defect concentrations on the reaction rates are also studied. This new approach can validate both the kinetic mechanisms and the appropriate kinetic coefficients, offering the potential to significantly reduce the uncertainty of the kinetic methodology and providing a powerful predictive tool for simulating irradiation behavior of nuclear materials.

KEYWORDS: Ab initio force-matching method; molecular dynamics; kinetic rate equations; multiscale approach.

1. INTRODUCTION

A vast literature exists on the properties of body-centered cubic (*bcc*) metals, including Mo and Mo alloys irradiated with neutrons, electrons, and ions [1–17]. Interstitials, vacancies, and rare-gas atoms contribute to lattice damage. The evolution of self-interstitial atoms (SIAs) and vacancies (VACs) is the first stage of defective structure relaxation in radiation cascade formation. This stage plays an important role in the nucleation process of the clusters of SIAs, dislocations, and voids. Modern kinetic theory of the radiation damage based on the diffusion-controlled reaction kinetics and mean field theory describes the kinetics of these processes in terms of diffusion coefficients and interaction radius of defects [7–13]. However, such a traditional approach cannot provide accurate values of both the kinetic coefficients and the defect interaction radii, which can depend on temperature. These parameters should specifically be addressed because of the complexity of mechanisms of SIA+SIA interactions and VAC+SIA interactions [14]. The mean field theory, for example, does not take into account the probability of binding of two defects into a bigger cluster, which in nucleation and chemical reaction theories is called a steric factor. This factor can be much less than unity, which is assumed in the existing radiation damage theory [7, 15–19].

A one-dimensional diffusion of SIAs and clusters of SIAs in Mo should be taken into account at low temperatures [20, 21]. A kinetic Monte Carlo study has shown that 1D diffusion can change the kinetics of the interaction between SIAs and sink strength dramatically [22]. A similar effect can be observed with SIAs and vacancies.

This paper describes molecular dynamics (MD) simulations of the evolution of a pure Mo system containing SIAs and vacancies. Included are results from investigating the influence of 1D diffusion on kinetics, as well as a description of the kinetics obtained by using an accurate,

*E-mail: insepov@anl.gov

newly developed Mo interatomic potential [23]. The paper presents a new multiscale approach that couples kinetic rate theory with ab initio and atomistic MD simulations. This approach allows one to bridge time and spatial scales from the quantum mechanical to the macroscopic world. A similar multiscale method was suggested by Stoller and Greenwood in 1998. They briefly explored using MD-simulated cross sections and proposed two approaches: a hybrid model that bridges different time and length scales ("handshaking") and an approach that involves passing information between models ("handing-off") [24]. In the present paper, an atomistic MD model of defect formation and annihilation is developed that addresses the evolution of the microstructure of Mo experiencing transient radiation cascade damage at the initial state and continuing until the stage where annealing of the defects becomes plausible.

2. SIMULATION METHOD

The point defects in an ideal *bcc* Mo crystalline structure were introduced into the system at the beginning of the simulation. The rate of damage generation during the defect evolution was set to zero.

Two types of initial defects were considered: crowdions and vacancies.[1] The initial space distributions of defects were uniform for both defect types. Crowdions have four equivalent directions in the basic crystal cell: [111], [$\bar{1}$11], [1$\bar{1}$1], and [11$\bar{1}$]. These equivalent orientations were assumed to be distributed uniformly. Such a simple MD model is applicable to simulation of the collision cascades at the initial cascade stage. The developed model is applicable to a quasi-equilibrium state for the defect sizes where the temperature and defect concentrations gradients were not too high.

Two types of initial microstructures were considered: a crystalline system containing only crowdions and a system with both crowdions and vacancies. Such an initial setup enables separate study of the kinetics of the cluster formation and recombination. The typical size of a simulation cell for the simulations of SIA+SIA reactions was 100×100×100 lattice units (31×31×31 nm) containing about 2×10^6 atoms. The initial numbers of crowdions were 300, 400, and 600. For evaluation of vacancy and SIA recombination rates, a 100×100×100 system with 200 crowdions and 800, 1000, 1500, and 2000 vacancies was used, and a 150×150×150 system with 200 crowdions and 3000, 4000, 5000, and 6000 vacancies was applied. During the calculation the vacancies were immobile. In all cases three-dimensional periodic boundary conditions were used.

First, the structure of the defects was optimized by minimizing the total potential energy. Then, the system was equilibrated at a given temperature and zero pressure. Equilibrium was reached in several picoseconds. A range of temperatures T = 300K, 400K, 600K, 800K, and 1000K was considered.

The interaction between atoms was described by the embedded atom method potential [23]. This potential was parameterized by an ab initio force-matching method, with a large set of configurations of the defects, and therefore was capable of reproducing a correct potential energy map and hierarchy of the formation and migration energies of the defects. The calculations were carried out by using the LAMMPS code [25].

Obtaining accurate kinetic rates with an MD method requires accurate diagnostic procedures for calculating the number of the defects in the studied systems. For this paper, the simulation was focused on several simple kinetic processes, such as defect recombination and di-

[1]We discuss these defects in detail in [23].

SIA formation. Therefore, diagnostic methods were developed to enable mapping interstitials, vacancies, di-SIAs, and clusters of di-SIAs. In order to increase the accuracy of the structure identification, certain steps were developed and then optimized, such as minimization of the total potential energy. This approach allowed the elimination of thermal fluctuations that could have obstructed the visual observation and overall accuracy of the method.

All defects were placed in a local environment where they could be characterized by the local variables (or parameters) that were sensitive to that environment. One such variable was the local coordination number (*CN*), which is the number of neighboring atoms within the sphere of a radius r_c. A typical value of r_c is $r_2 + r_3$, where r_2 and r_3 are the radii of the second and third coordination spheres, respectively. This local parameter was also applicable for studying the vacancies.

The centro-symmetry (*CS*) parameter was used as a second local variable; it characterizes the symmetry of the local environment. The variable obtained by common-neighbor analysis (*CNA*) was used as a third local parameter that recognizes the symmetry of the lattice: *hcp*, *bcc*, *fcc*. The local potential energy (*PE*) of the atom was used as a fourth local parameter.

3. RESULTS

We discuss here various types of defects—including crowdions, dumbbells, di-SIAs, and vacancies—observed in our simulations.

3.1 Point Defects in Mo

An SIA in Mo has two stable structural forms: a crowdion and a dumbbell. These defects have the lowest energy and therefore are the most stable SIA defects. Because they have almost identical potential energies, these defects are able to transform into each other by a one-dimensional motion. We note that a dumbbell defect formed along a <110> direction (a rotation form) was not taken into account since such a defect has a larger energy E_{D110}-E_{D111}~0.27eV [23] and exists for only a very short time.

The structure of the crowdion consists of one additional Mo atom in the *bcc* cell along the <111> diagonal. The energy minimization of this structure results in expanding the lattice along the <111> direction.. The number of atoms with a maximum value of the energy was equal to the number of crowdions, and therefore the direction of the SIA chain was parallel to the direction of the motion.

A similar idea was used to identify the <111> dumbbell form. The <111> dumbbell was characterized by two atoms symmetrically located around the center of the basic cell. The *PE* parameter is not sufficient to correctly identify the defects in a crystal with a large diversity of defect types. Therefore, the *CS* parameter was used, in addition to the *PE* local parameter. The values of these parameters are shown in Table 1.

Table 1: Diagnostics parameters for different defect structures.

Type	**Crowdion**	**Dumbbell**	**di-SIAmob1**	**di-SIAmob2**	**di-SIAsessile**	**Vacancy**
PE, eV	> -5.4	(-5.8..-5.4)	(-6.6..-6.0)	(-5.9..-5.5)	> -6.0	< -6.6
CS	< 2	< 3	(8.5..9.1)	< 2	(7.6..8.5)	(6..8)
CN	> 14.5	> 14.5	> 14.5	> 14.5	> 14.5	< 13.5

Two stable types of di-SIAs were observed. The first one is the mobile configuration, which can be represented by two parallel interstitials. The mobile configuration can change

during the motion to another, a sessile cluster configuration. It forms when the two additional atoms appear in the same elementary *bcc* cell. The atoms are redistributed in symmetrical positions. The equilibrated configuration in terms of *PE* looks like a star but is not flat. The directions of the cluster atoms are [111], [11 $\bar{1}$], and [1 $\bar{1}$ 1]. There is also another equivalent direction, [$\bar{1}$ 11], where the transition from the initial direction to an empty direction was also observed during the simulations. Cross-configuration is characterized by the three central atoms. Vacancies are identified by *PE* and *CS*. As an additional condition the *CN* parameter is used, with $CN < 13.5$, because the ideal lattice has 14 neighbors in a sphere of radius $(r_2 + r_3)$. Eight atoms of the vacancy environment correspond to one vacancy.

The main objective of our investigation of the mechanisms was to obtain the relative favorable configurations of defects that result in the reaction and the reaction distance (interaction radius). The main reaction path of the mobile di-SIA formation is the interaction between the two parallel crowdions or dumbbells close to each other. The distance of interaction R_0 is about $\sqrt{3}a_0$. The sessile di-SIAs are formed mainly by the interaction of two crowdions on the concurrent lines along three other equivalent axis. But the formation from two parallel crowdions is observed also.

The mechanisms of the formation of the two types of di-SIAs are closely interlaced. Two parallel crowdions can form a sessile di-SIA, and two conjugate crowdions can form a mobile one. The interaction distance between the concurrent and conjugate SIAs is larger than that of the parallel configurations. The sessile di-SIA can rearrange to the mobile form during the simulation. The reason is that the mobile form has a lower formation energy (about 0.4 eV) than does the sessile form, as observed in [23].

If the system contains both vacancies and SIAs, recombination (annihilation) between these two defect types is observed. The main conclusion from the observation of SIA+SIA and VAC+SIA reactions is that the reaction distance is very high: it can reach 10 Å.

3.2. Kinetic Rate Theory

The following basic rate equations describe the kinetics of the system of defects with the number densities c_i and c_v [7]:

$$\begin{aligned} \frac{dc_i}{dt} &= G - \alpha_r c_v c_i - k_i D_i c_i - \sqrt{2} D_i c_i c_i / \Omega^{2/3} + 2\Omega^{1/3} b_v D_v c_v n_l / \pi d_l, \\ \frac{dc_v}{dt} &= G - \alpha_r c_v c_i - k_v D_v c_v - 2\Omega^{1/3} b_v D_v c_v n_l / \pi d_l, \end{aligned} \tag{1}$$

where $c_{i,v}$ are the concentrations of interstitials and vacancies; G is the damage rate in *dpa*/*s*; α_r is the self-interstitial-vacancy recombination coefficient; b_v and Ω are the Burgers vector and the atomic volume, respectively; and D_α ($\alpha = v$, i) is the diffusion coefficients of vacancy, interstitial, and gas atoms; and k_α ($\alpha = v$, i) are the vacancy/interstitial sink strengths, where k_a include fission gas bubbles, Frenkel pairs, clusters, and dislocations. The rate equations can be solved by direct numerical integration or, in limited cases, by a simple analytical solution. Our MD model was constructed by simplifying the rate equations and by setting the rate G to zero. Since the diffusion coefficient of vacancies, D_v, was much lower than that for interstitials, D_i, for the whole simulation time and for all temperature ranges the interstitials and vacancies were considered as absorbed voids with radius equal to the interaction radius.

A big difference exists between 1D and 3D diffusion of SIAs. Our simulation uses 3D diffusion at high temperatures and 1D diffusion at low temperatures. At 300K the typical time of the 1D diffusion is several nanoseconds, and the mean free path length is about 30 nm [26].

A "hedgehog" model is proposed to explain the complex anisotropic character of interactions between self-interstitials and vacancies in Mo. The model was applied to study the annihilation of self-interstitials with vacancies.[2] According to this model, SIAs move almost freely along four equivalent directions <111>. Therefore, if a Frenkel pair of SIA + VAC defects occupies the same <111> axis and if the defects are closer than a certain recombination distance, they spontaneously annihilate. Our MD calculations have shown that the number of such spontaneous sites in a *bcc* Mo lattice near the vacancy ranges from 42 to 50, located along the four equivalent <111> directions around the vacancy. An effective isotropic radius of a sphere around the vacancy comprising the same number of lattice nodes would be $2a_0$.

An important feature of this model is that the interaction radius depends on temperature. The conventional isotropic interaction radius theory of Frenkel pair recombination [27] also shows that the radius of interaction of a long-range isotropic elastic field near the vacancy can depend on temperature. In *bcc* Mo, however, the two types of migration of defects differ significantly. Specifically, *1D* migration along the <111> axis is almost free: the activation energy of 1D migration is of about 0.02 eV, which is less than the accuracy of the ab initio method used to calculate this value. On the other hand, *3D* migration needs a much higher activation energy, ~ 0.3 eV [23], which makes this model more complex and adds a new temperature dependence.

To simplify the analysis, we describe the kinetics in terms of *3D* diffusion, but we take into account the dependence of the constant rate on temperature. This approach allows us to investigate the transition from *3D* to *1D* diffusion. Equation (1) then can be simplified:

$$\frac{dc_i}{dt} = -\alpha_r c_i c_v - \alpha_{ii} c_i c_i, \qquad \frac{dc_v}{dt} = -\alpha_r c_i c_v. \tag{2}$$

Here α_r and α_{ii} are the rate constants in terms of the binary reactions; $\alpha_{ii} = \sqrt{2} D_i / \Omega^{2/3}$ is the rate constant for association of two SIAs into one di-SIA. Equation (2) can be solved analytically in order to compare with MD results.

Figure 1 illustrates the evolution of the number of interstitial atoms and di-SIAs. During the first 10 ps the system reaches quasi-equilibrium state, where the temperature and pressure are equilibrated and the very close interstitials interact by forming clusters of interstitials. The diagnostics is verified by the total number of recognized defects, N_{total}, equal to *NSIA* + *Ndi-SIA*. If N_{total} equals N_0, the diagnostics accurately recognizes all defect structures. After a long calculation time the N_{total} changes, indicating that three SIAs and larger clusters are formed.

[2] Although this model should be applicable to di-SIA formation, we didn't try to use it for this purpose.

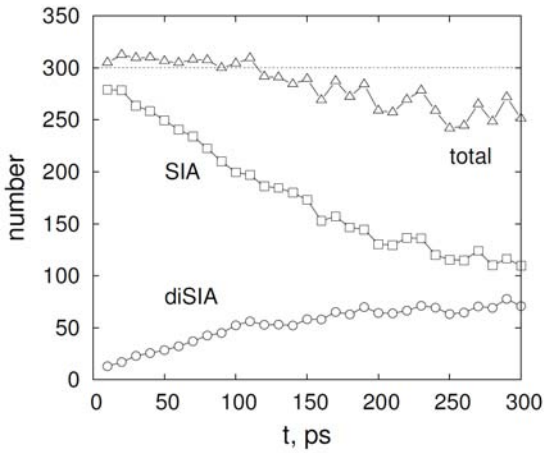

Figure 1: Number of SIAs and di-SIAs, and total number of recognized defects. The system size is 2 million atoms, and T = 1000K.

Integration of Eq. (2) gives the following analytic solution:

$$1/c_i - 1/c_{i0} = \alpha_{ii} t, \qquad (3)$$

enabling comparison of our MD results with the kinetic theory to be made in the coordinates $1/c_i - 1/c_{i0}$ vs t , in order to obtain the rate constant.

Figure 2 shows the evolution of defect concentrations obtained by MD at three initial concentrations of vacancies at 300K. Figure 3 shows the rate dependencies, approximated by the linear equation with the slope α_{ii}., which was independent of the initial concentration. One can conclude that the reaction is second order at both temperatures, although the motion is strongly 1D at T = 300K and mostly 3D at T=1000K.

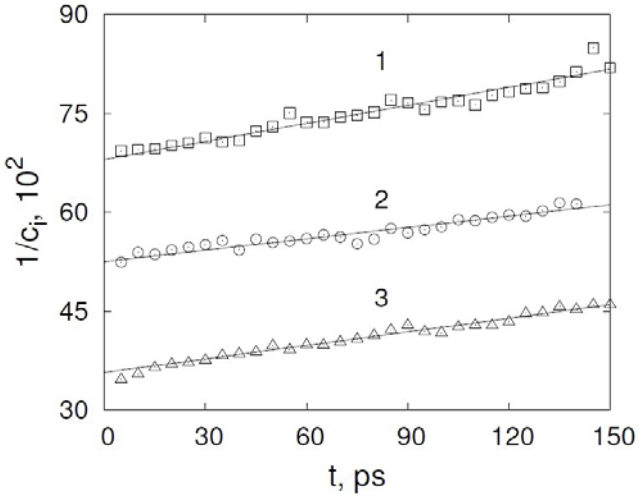

Figure 2: Dependence of the SIA number on time for different initial concentrations c_{i0}: 1 –1.5*10^{-4}, 2 – 2*10^{-4}, 3 – 3*10^{-4}. T=300K.

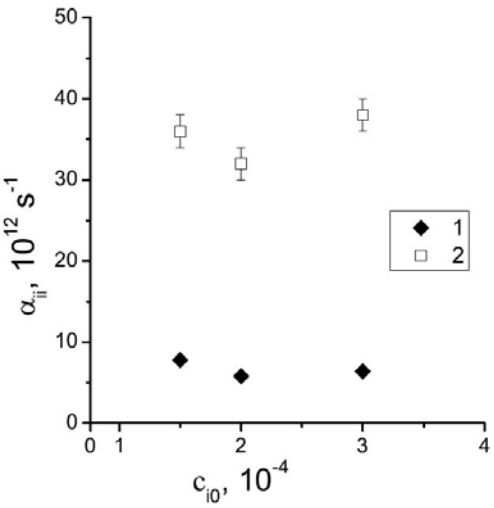

Figure 3: Dependence of rate constant α_{ii} on the initial concentration for two temperatures *T*: 1 – 300K, 2 – 1000K. The system size is 2 million atoms.

Figure 4a shows the evolution of mobile and sessile clusters in the di-SIA system containing an equal number of self-interstitials and no vacancies. An interesting feature of this plot is that the number of sessile clusters saturates after about 30 ps, whereas the number of mobile clusters is still growing. This illustrates the stability of sessile clusters, which we believe are the nuclei of the larger dislocation loops since they become larger as the evolution continues. We will test this assumption by comparing the concentration of the sessile clusters with experimental density of dislocation loops in Mo irradiated by electrons [28].

Figure 4b shows that the relative number of sessile cluster become less at *T*=1000K, which characterizes thermal resolution of the sessile and larger clusters into mobile ones. The estimated binding energy of the sessile clusters is 0.2 eV.

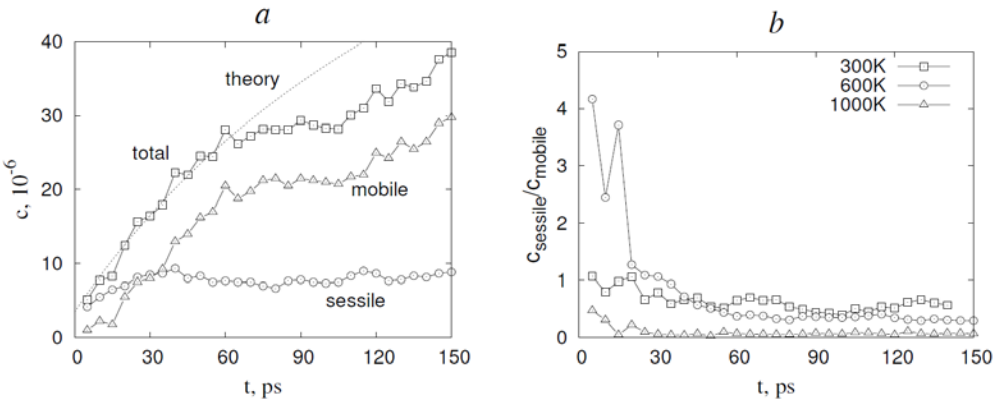

Figure 4: (a) Dependence of the number of different types of di-SIAs on time *T*=600K; (b) dependence of the ratio of the immobile configuration of di-SIAs on time for three temperatures: *T*=300K, *T*=600K, *T*=1000K. The system size is 2 million atoms.

3.3. Determination of Rate Constants

The rate constants of the SIA+SIA and VAC+SIA reactions were calculated at different temperatures by using molecular dynamics. The results were then compared with the theoretical values used in kinetic rate methodology.

3.3.1. SIA+VAC Reactions

The recombination rates of SIA+VAC reactions were determined from MD simulation data by using Eq. (3). The system, containing from 2×10^6 to 6×10^6 molybdenum atoms, was injected with 200 SIAs and 1,000 vacancies. The concentrations of interstitials were fitted according to the solutions of the kinetic equations (2) and (3). Figure 5 shows the results of fitting the analytical solution (3) to MD results at five temperatures, which determine the rate constants. Similar fitting procedures were conducted at several initial concentrations of vacancies, to be sure that the results do not depend on the initial concentration of vacancies.

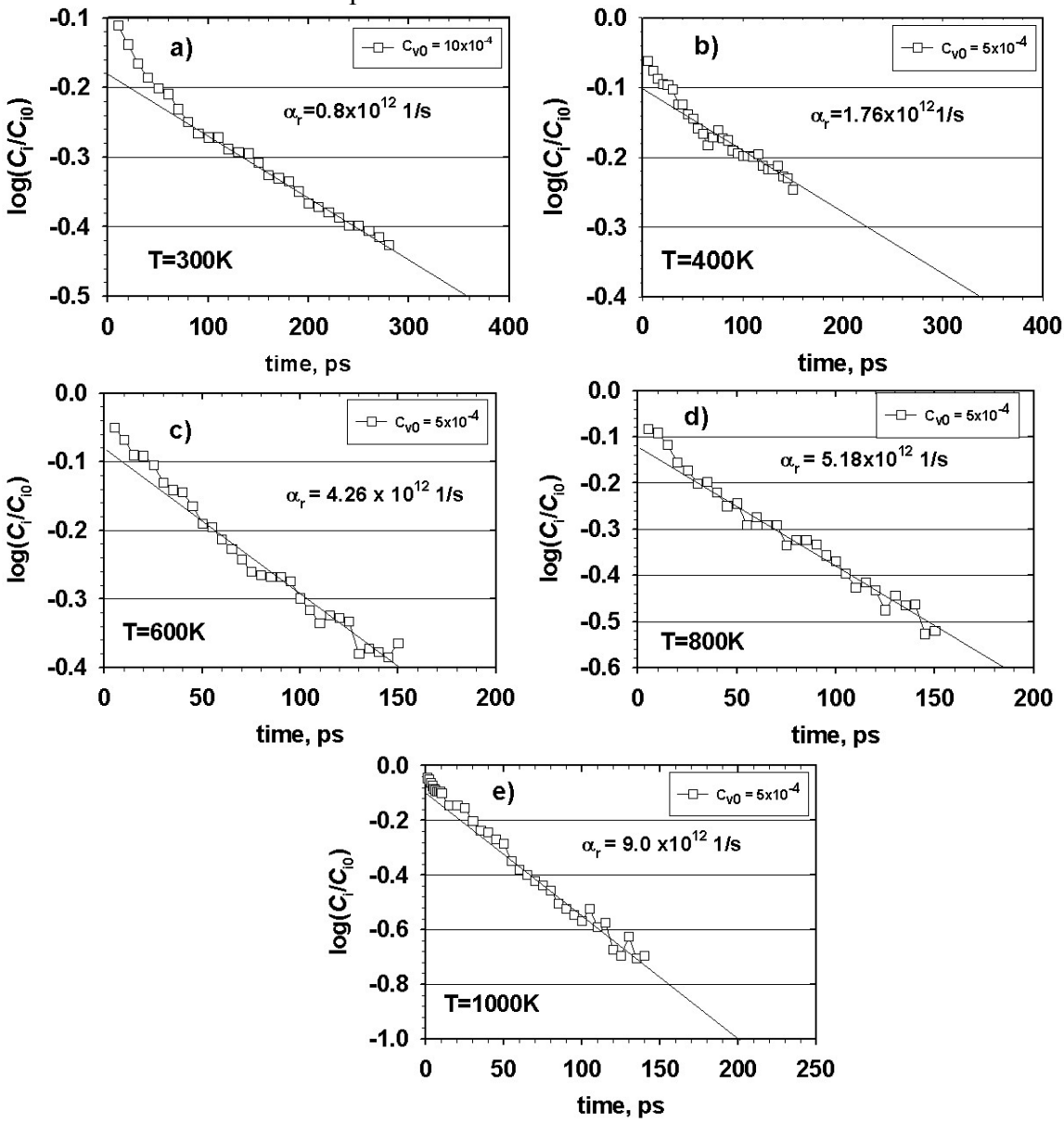

Figure 5: Calculation of the rate constants α_r of annihilation between interstitials and vacancies at five temperatures obtained by MD in this work: (a) T = 300K, (b) T = 400K, (c) T = 600K, (d) T = 800K, and (e) T = 1000K.

Recombination rate constants for the reactions between interstitials and vacancies can be obtained as follows [7]:

$$\alpha_r = 4\pi R_0 (D_i + D_v)/\Omega \approx 4\pi R_0 D_i / \Omega, \quad (4)$$

where R_0 is a constant recombination radius, which usually is set to a lattice parameter. In [29], the recombination radius was obtained from resistivity experiment to be between 0.7 and 2.5a_0 for molybdenum. Our Frenkel pair recombination model assumes that the recombination radius can be a temperature-dependent value, $R_1(T)$:

$$\alpha_r = 4\pi r_{iv} (D_i + D_v)/\Omega \approx 4\pi r_{iv} D_i / \Omega, \quad (5)$$

where $r_{iv} = R_0 + R_1(T)$, R_0 is the constant radius with a typical value at low temperatures, and R_1 is the temperature-dependent term, which we set as an Arrhenius expression with the 3D activation energy barrier:

$$R_1(T) = \xi \exp\left(-E_a^{3d}/kT\right). \quad (6)$$

Here, $\xi = 0.125$ is the steric factor that takes into account eight possible ways for an interstitial hopping from one gliding direction to another. The diffusion coefficient of interstitials, D_i, is determined by 1D diffusion,

$$D_i = D_0 \exp\left(-E_a^{1d}/kT\right), \quad (7)$$

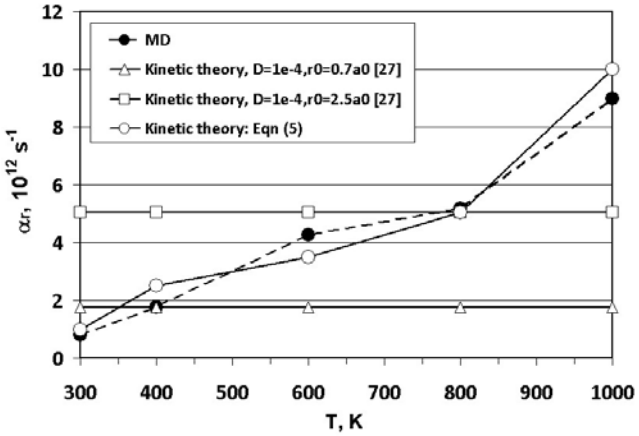

Figure 6: Dependence of the recombination rate constant of SIA+VAC reaction on temperature: solid circle – our MD results; open triangle and squares – equation (4) with $D = 1\times10^{-4}$ cm^2/s and R_0 = 0.7 and 2.5 a_0, where a_0 is the Mo lattice parameter [7]; open circles and solid line – equation (5).

and Figure 6 plots various approximations that determine the temperature dependence of the Frenkel pair recombination rate constant α_r given by Eqs. (5)–(7).

3.3.2. SIA+SIA Reactions

Several formulas are given in the literature for determining the SIA + SIA association rate constant based on the theory of diffusion-limited reactions [7, 10-13]. A simple approximation of the rate constant can be made by an Arrhenius formula:

$$\alpha_{ii} = \alpha_{ii0} \exp(-E_a / kT), \quad (8)$$

where α_{ii0} is the pre-exponential constant, E_a the activation energy, and T the temperature. The parameter α_0 can be obtained from the following requirement: $\alpha(300\text{K}) = \alpha_{MD}(300\text{K})$. The best fit between the kinetic coefficients approximated by (8) is obtained with the activation energy E_a = 0.072 eV.

Theoretical values of the rate constants for the SIA+SIA interaction can also be obtained by the conventional formula (see, e.g., [7] for more detail)

$$\alpha_{ii} = \sqrt{2} \cdot D_i(T) / \Omega^{2/3}, \quad (8)$$

where $D_i(T)$ is the SIA diffusion coefficient depending on temperature and Ω is the atomic volume. The dependence $\alpha(T)$ can be taken into account just by the dependence $D(T)$. This gives the following approximation formula:

$$\alpha_{ii} = \frac{\sqrt{2}}{\Omega^{2/3}} \cdot D_{MD}(T) / D(300K), \quad (9)$$

which, together with Eq. (8) (with slight modification), has been applied to analyze 3D point defect diffusion (see, e.g., [7]). However, previous studies have not taken into account the significantly anisotropic 1D behavior of defect migration in irradiated *bcc* Mo at low and intermediate temperatures. When one does take into account the almost free movement of SIAs inside the "needles" of the hedgehog model (i.e., the MD result that self-interstitials in the *bcc* lattice are moving along four equivalent directions almost without activation energy [26]), one obtains the following expression, where the exponential dependence is enhanced by a stronger power dependence on T:

$$\alpha_{ii}^{1d} = \frac{2\sqrt{2}}{\Omega^{2/3}} D_i^{1d} = \xi \frac{2\sqrt{2}}{\Omega^{2/3}} \cdot AT^s \exp\left(-E_a^{3d} / kT\right), \quad (10)$$

where A, s are the adjustable parameters and ξ is the steric factor.

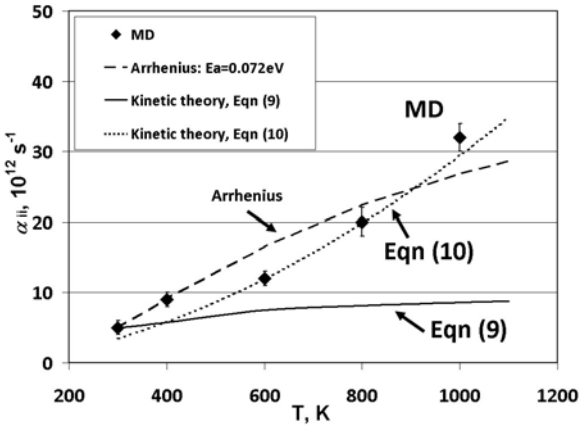

Figure 7: Dependence of the rate constant of SIA+SIA reaction on temperature: diamond symbols – our MD results; dashed line – Eq. (1) with E_a = 0.072 eV; solid line – Eq. (9). Our new model is shown by a dotted line drawn by Eq. (10) and has correct curvature fitting the MD results.

Figure 7 shows a comparison of the MD results with kinetic theory, where the kinetic theory coefficients were obtained by using Eqs. (7)–(9). The figure shows that the expressions (8) and (9), applicable to the conventional 3D diffusion mechanism and widely used in kinetic rate theory, fail to satisfactorily describe the MD results. In particular, they give the wrong asymptotic behavior: the Arrhenius dash and the kinetic rate theory solid lines saturate at higher temperatures, whereas the MD data shows a much faster growth. Adding a power dependence to pre-exponential according to Eq. (10) significantly improves the comparison and changes the character of curve to a growing type that fits the MD data.

3.4. Comparison of Sessile Cluster Concentration with Experiment

The concentration of the immobile sessile clusters saturates with time (see Fig. 4a), whereas the concentration of mobile clusters continues to grow. This situation means that the sessile clusters will most probably grow in size after they reached an equilibrium concentration. Our MD diagnostic procedure cannot reveal sessile clusters larger than a dimer. Therefore, we did a preliminary comparison of the calculated concentration of sessile clusters with the experimental density of small dislocation loops observed in Mo irradiated by electron bombardment [28].

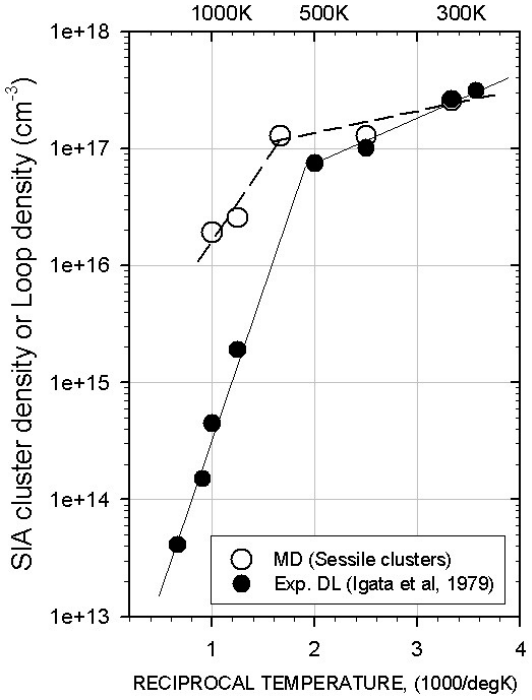

Figure 8: Comparison of the concentrations of sessile clusters obtained by MD in this work with experimental dislocation loops density in [28].

Our preliminary results, plotted in Fig. 8, show that the sessile clusters can become nuclei of the dislocation loops in irradiation experiments, since they do not change their concentration after reaching equilibrium in the system at any given temperature.

4. SUMMARY

In previous work, molecular dynamics and Monte Carlo methods were successfully used to calculate kinetic coefficients for cluster formation processes in rarefied gas and in dense media [30]. In the present paper, a multiscale concept is proposed for simulating the evolution of

radiation defects in Mo. The new concept, which is applicable to nuclear materials damaged by radiation, consists of using atomistic simulation methods to study radiation damage, defect formation, and growth processes and to calculate the probabilities of elemental processes and reactions that are applicable to irradiated nuclear materials. Since interaction potentials are important for the new concept, a new Xe-Mo interatomic potential was developed by using an ab initio force-matching method [26]. This potential was then used to study defect mobility, accumulation, and diffusion.

MD simulations were conducted for SIA+SIA and VAC+SIA reactions, which play a crucial role in the initial stages of radiation damage. Specifically, the influence of 1D diffusion on kinetics was considered by using simulation at different temperatures. Although the diffusion of SIAs is strongly one dimensional at $T = 300$K, the reaction of SIA+SIA is described as a second-order reaction also at high temperatures. The same conclusion is drawn for the recombination of vacancies and SIAs.

The rate constants of SIA+SIA and VAC+SIA reactions also were calculated based on the kinetics, and the temperature dependencies were obtained. Comparisons indicate that the kinetic theoretical values are much smaller than the MD results.

Acknowledgments
This work was supported by the U.S. Dept. of Energy under Contract DE-AC02-06CH11357.

REFERENCES

[1] J. H. Evans, Observations of a regular void array in high purity molybdenum and T.Z.M. irradiated at high temperatures with 2MeV nitrogen ions, Rad. Eff. 10 (1971) 55–60.
[2] S. L. Sass, B. L. Eyre, Diffraction from void and bubble arrays in irradiated molybdenum, Phil. Mag. 27 (1973) 1447–1453.
[3] V. K. Sikka, J. Moteff, Damage in neutron-irradiated molybdenum, J. Nucl. Mater. 54 (1974) 325–345.
[4] C. Templier, Inert gas bubbles in metals: A review, in Fundamental Aspects of Inert Gases in Solids, ed. S. E. Donnelly and J. H. Evans, Plenum Press, N.Y., 1991, 117–132.
[5] P. B. Johnson, Gas bubble lattice in metals, in Fundamental Aspects of Inert Gases in Solids, ed. S. E. Donnelly and J. H. Evans, Plenum Press, N.Y., 1991, 167–184.
[6] D. J. Mazey, B. L. Eyre, J. H. Evans, S. K. Erents, G. M. McCracken, A transition electron microscopy study of molybdenum irradiated with helium ions, J. Nucl. Mater. 64 (1977) 145–156.
[7] J. Rest, An alternative explanation for evidence that xenon depletion, pore formation, and grain subdivision begin at different local burnups, J. Nucl. Mater. 277 (2–3) (2000) 231–238.
[8] C. Domain, C. Becquart, L. Malerba, Simulation of radiation damage in Fe alloys: An object kinetic Monte Carlo approach, J. Nucl. Mater. 335 (1) (2004) 121–145.
[9] C. Becquart, C. Domain, U. Sarkar, A. DeBacker, M. Hou, Microstructural evolution of irradiated tungsten: Ab initio parameterization of an OKMC model, J. Nucl. Mater. 403 (1–3) (2010) 75–88.
[10] G. Dienes, A.C. Damask, Kinetics of vacancy-interstitial annihilation. II. Di-interstitial formation, Phys. Rev. 125 (1962) 447–450.
[11] R. Nozato, T. Yamaji, Kinetics of precipitation in a Pb-0.068 wt% Ag alloy, Trans. JIM 21 (1980) 131-139.

[12] N. Ghoniem, D.D. Cho, The simultaneous clustering of point defects during irradiation, Phys. Stat. Sol. 54 (1979) 171–178.
[13] N. Ghoniem, S. Sharafat, A numerical solution to the Fokker-Planck equation describing the evolution
of the interstitial loop microstructure during irradiation, J. Nucl. Mater. 92 (1980) 121–135.
[14] B. Grant, J. Harder, D. Bacon, Interstitial-vacancy recombination for model bcc transition metals, J. Nucl. Mater. 171 (2-3) (1990) 412–414.
[15] R. Sizmann, The effect of radiation upon diffusion in metals, J. Nucl. Mater. 69 & 70 (1968) 386–412.
[16] A.D. Brailsford, R. Bullough, the rate theory of swelling due to void growth in irradiated metals, J. Nucl. Mater. 44 (1972) 121–135.
[17] M. Kiritani, Analysis of the clustering process in supersaturated lattice vacancies, J. Phys. Soc. Jpn. 35 (1973) 95–107.
[18] M. R. Hayns, The nucleation and early growth of interstitial dislocation loops in irradiated materials, J. Nucl. Mater. 56 (1975) 267–274.
[19] M. H. Yoo, Dislocation loop growth and void swelling in bounded media by charged particle damage, J. Nucl. Mater. 68 (1977) 193–204.
[20] S. Han, L. A. Zepeda-Ruiz, G. J. Ackland, R. Car, D. J. Srolovitz, Self-interstitials in V and Mo, Phys. Rev. B 66 (22) (2002) 220101.
[21] P. M. Derlet, D. Nguyen-Manh, S. L. Dudarev, Multiscale modeling of crowdion and vacancy defects in body-centered-cubic transition metals, Phys. Rev. B 76 (5) (2007) 054107.
[22] H. Heinisch, H. Trinkaus, B. Singh, Kinetic Monte Carlo studies of the reaction kinetics of crystal defects that diffuse one-dimensionally with occasional transverse migration, J. Nucl. Mater. 367–370 (2007) 332–337.
[23] S. V. Starikov, A. Y. Kuksin, Z. Insepov, J. Rest, V. Stegailov, G. Norman, Radiation defects by Xe ion implantation and the evolution of self-interstitial atom clusters in molybdenum, Preprint ANL/MCS-P1788-0810, Mathematics and Computer Science Division, Argonne National Laboratory, 2010.
[24] R. E. Stoller, L. R. Greenwood, From molecular dynamics to kinetic rate theory: A simple example of multiscale modeling, ORNL/CP-10122, in Proc. of MRS 1998 Fall Meeting, Symp. J: Multiscale Modeling of Materials, Boston, 1998.
[25] S. J. Plimpton. Fast parallel algorithms for short-range molecular dynamics, J. Comp. Phys. 117 (1995) 1–19.
[26] Z. Insepov, J. Rest. G. L. Hofman, A. Yacout, A. Yu. Kuksin, G. E. Norman, S. V. Starikov, V. V. Stegailov, A. V. Yanilkin, A new multiscale approach to nuclear fuel simulations: Atomistic validation of the kinetic method, Trans. Am. Nucl. Soc., vol. 102, San Diego, 2010.
[27] K. Schroeder, K. Dettmann, Diffusion Reactions in Long Range Potentials, Z. Phys. B 22 (1975) 343–350.
[28] N. Igata, A. Koyama, K. Itadani, Radiation effects on molybdenum alloys bombarded by electrons in a high-voltage electron microscope, Eff. Rad. Struct. Mater., ASTM STP 683, edited by J. A. Sprague and D. Kramer, Am. Soc. Test. Mater., 1979, pp. 12–31.
[29] H. B. Afman, Stage I recovery of molybdenum irradiated at 4.2°K with electrons of different energies, Phys. Stat. Sol. A11 (1972) 705–712.
[30] Z. Insepov, E. M. Karataev, G. E. Norman, The kinetics of condensation behind the shock front, Z. Phys. 20 (1991) 449–451.